



# Chemopreventive Potential of a Phytofabricated Silver Nanoformulation using Bark Extract of *Saraca asoca* in AML Mice *In vivo* and *In vitro*

Pratyusha Banerjee; Puspendu Roy; Debjani Nath\*

Department of Zoology, University Of Kalyani, Kalyani Nadia, West Bengal, India.

\*Corresponding Author(s): Debjani Nath

Department of Zoology, University Of Kalyani,  
 Kalyani Nadia, West Bengal, PIN 741235, India.  
 Email: nath\_debjani@yahoo.co.in

## Abstract

**Objectives:** To evaluate the therapeutic potential of phytofabricated silver nanoparticle reduced by bark extract of *Saraca asoca* for Acute Myeloid Leukemia (AML).

**Methods:** The efficacy of silver nanoformulation was tested *in vivo* secondary model of AML in comparison to chemotherapeutic drug doxorubicin and the cytotoxic and genotoxic potential of the nanoparticle *in vitro* in leukemic cells in comparison to normal lymphocytes.

**Results:** Both these approaches proved that AgNPs were selectively cytotoxic towards leukemic lymphocyte cells through oxidative damage, which were comparable to the standard chemotherapeutic drug.

**Conclusions:** This finding opens a new avenue for the biomedical application of environmentally sustainable green phyto-fabricated AgNPs in chemoprevention of AML.

Received: Mar 26, 2021

Accepted: Apr 22, 2021

Published Online: Apr 26, 2021

Journal: Journal of Nanomedicine

Publisher: MedDocs Publishers LLC

Online edition: <http://meddocsonline.org/>

Copyright: © Nath D (2021). This Article is distributed under the terms of Creative Commons Attribution 4.0 International License

**Keywords:** Acute myeloid leukemia; Silver nanoparticle; Green synthesis; Chemoprevention; Genotoxicity; cytotoxicity.

## Introduction

Acute Myeloid Leukemia (AML) is one of the most complex types of leukemia, which needs new and advanced mode of treatment. The impaired production of myeloid blood cells or pancytopenia of AML leads to the reduction of erythrocytes, lymphocytes and platelets. AML occurs due to exposure to agents like smoking, certain chemicals like alkylating agents, platinum and benzene, certain blood diseases, genetic disorders, exposure to radiations etc.

In contrast to the conventional treatment like chemotherapy, radiotherapy and stem cell transplantation, plant phytochemicals can be used as nontoxic chemopreventive agent to provide long-term therapeutic effect [1-5].

Several reports are now available on the anticancer activity of the silver nanoparticles synthesized by green chemistry method. According to Prabhu et al. [6] green-synthesized AgNPs by methanolic extract of *Vitex negundo* L. showed 50% inhibition of cell viability of Human Colon Cancer Cell Lines (HCT 15). The cytotoxic properties of biologically synthesized silver nanoparticles from *Acalypha indica* was observed in human breast tumor cells, MDA-MB-231 [7,8]. AgNPs from *Andrographis echinoides* inhibited the growth of human breast adenocarcinoma cells [9]. Additionally, biofunctionalized green-synthesized AgNPs exhibited potential cytotoxic activity against HT29 human colon adenocarcinoma cells [10]. AgNPs bioformulated

**Cite this article:** Benerjee P, Roy P, Nath D. Chemopreventive potential of a phytofabricated silver nanoformulation using bark extract of *Saraca asoca* in AML mice *in vivo* and *in vitro*. J Nanomed. 2021; 4(1): 1036.



by using *Premna serratifolia* leave extract displayed significant anticancer activity on liver cancer of Swiss albino mice [11]. Sre et al. [12] reported the cytotoxic activity of phytochemically synthesized AgNPs from *Erythrina indica* on MCF-7 (breast cancer) cells and HepG2 (hepatocellular carcinoma) cells. Another group of scientists reported the AgNPs, synthesized using the latex of *Euphorbia nivulia*, exhibited potentially cytotoxic effects in a dose-dependent manner against human lung carcinoma (A549) cells (Sukumar et al. 2013) [13]. *Annona squamosa* seed extract displayed good anticancer activities against human hepatoma and breast cancer cells both *in vitro* and *in vivo* [14,15]. The anticancer efficacy of *Allium sativum* (garlic) exerted the protective effect against gastrointestinal cancers [16] and administration of garlic enhanced the efficacy of natural killer cells in patients with advanced digestive system cancer [17]; Curcumin, a polyphenol (diferuloylmethane) derived from the rhizome of turmeric (*Curcuma longa* Linn), is a strong anticancer agent showed its multiple actions on mutagenesis, cell cycle progression, apoptosis, oncogene expression, and metastasis [18]. According to the study of Dhillon et al. [19], curcumin showed positive results in pancreatic bladder cancer patients too. So it is quite evident that the silver nanoparticles capped with phytocomponents with medicinal value have a great prospect of utilization as a new line of treatment in acute myeloid leukemia. A few reports are available on anti-leukemic activity of silver nanoparticles in acute myeloid leukemia cells [20,21,22].

The plant *Saraca asoca* is a rain-forest tree belonging to the family Caesalpinaceae. It is native of Asia and South America. In India it is distributed throughout central areas of Deccan plateau and Western Ghats of the subcontinent. The bark of *Saraca asoca* has natural detoxification properties, rich in different phyto-compounds that have usages in the treatment of health issues like bleeding disorders, menorrhagia, and diarrhea, even in control of obesity. In this study we have analyzed the efficacy of the phytofabricated silver nanoparticle using the bark extract of *Saraca asoca* as reducing agent against the secondary AML mice model both *in vivo* and *in vitro* in comparison to common anticancer drug doxorubicin.

## Materials and methods

### Chemicals

Osmium tetroxide, Glutaraldehyde (electron microscopy grade), DAPI (4', 6-Diamidine-2'-phenylindole dihydrochloride), DCFDA dye, histopaque, doxorubicin (purchased from Sigma Aldrich chemical company, Mumbai, India). Annexin V-FITC Apoptosis Detection Kit was purchased from Invitrogen, Thermo Fisher Scientific (Mumbai, India).

### Animals

Swiss albino male mice (*Mus musculus*) of the age group of six to eight weeks from specified strain were purchased from a registered supplier. All the animals were maintained and treated as per direction and approval of the Institutional Animal Ethics committee, Department of Zoology University Of Kalyani (892/Go/Re/S/01/CPCSEA, dated 28.04.2014), (registered to Committee for the purpose of control and supervision of experiments on animals (CPCSEA), Ministry of Environment and, Forest and Climate Change, Animal Welfare Division, Government of India,) in stainless steel wire cages (Tarsons, India) under 12 hour light-dark cycle. Pellet diet (West Bengal Dairy and Poultry development corp. Ltd., Kalyani Industrial Area, Kalyani, WB In-

dia) was provided and water was supplied *ad libitum* automatically through the tubing during the study period.

### Secondary acute myeloid leukemia (AML) mice model

The secondary AML mice model was developed following the methodology of Saha et al. [23]. To develop the secondary AML model liquid benzene (HPLC grade) (MERCK, India) was vaporized by heating at 16°C and then the vapor was channeled into the inhalation chamber (1.3m<sup>3</sup>). A total of four groups (each containing six mice) were taken for the experimental (AML group) process. All the groups were exposed to 300 ppm benzene (in vapor form) for 6 h/day, 5 days/week for 2 weeks. Cumulative exposure= ppm X no of hours X no of days. Temperature and humidity were maintained automatically at 24 ± 1°C and 55 ± 10% respectively inside the chambers.

### Green phyto-fabricated silver nanoparticle

Green phyto-fabricated silver nanoparticles were synthesized using aqueous bark extract of *Saraca asoca* as the reducing agent [24]. The taxonomic identification of plant material was confirmed by Dr G. G. Maity, Professor of Taxonomy, Taxonomy and Plant systematic unit, Department of Botany, University Of Kalyani. The voucher specimens (Deb.kly-60) was deposited and preserved in the Department of Botany. The LD50 of the synthesized silver nanoparticle was 2165mg/kg body weight (Table 1). Two selected doses (for *in vivo*) were 43mg/kg b.w and 86mg/kg b.w. which were actually the 1/50<sup>th</sup> and 1/25<sup>th</sup> fraction of the determined LD50 of the green silver nanoparticle. Doses were selected as per the guidelines of OECD (2001) [25].

**Table 1:** LD5 to LD90 values of synthesized silver nanoparticle.

Percentile	Probit	Dose (mg/kg) Mean ± SEM
5	3.36	720.02 ± 330.51
10	3.72	908.05 ± 358.37
20	4.16	1142.45 ± 398.48
30	4.48	1403.09 ± 412.11
40	4.75	180936 ± 421.15
50	5.00	2165.26 ± 452.17
60	5.25	2673.28 ± 491.44
70	5.52	3113.51 ± 615.91
80	5.84	3768.40 ± 903.93
90	6.28	5322.89± 1647.36

### Study of anti-leukemic activity of phyto-fabricated silver nanoparticle in secondary AML Mice model

**Experimental Design:** The treatments (the synthesized silver nanoparticle and the standard drug) were given by i.p. injection at every second day upto 30 days. Overall survival was registered during the 35<sup>th</sup> day of the study. The groups were I: Control: normal healthy mice without any disease and received no treatment; II: AML mice received no treatment; III: AgNPs treated AML mice treated with 43mg/kg b.w. of AgNPs; IV: AgNPs treated AML mice treated with 86mg/kg b.w. V: AML mice model treated with 2mg/kg b.w. of doxorubicin.

**Survivability Assay:** The study was conducted for a period of total 35 days. Kaplan-Meier (1958) [26] analysis was performed

to determine the *in vivo* survival distributions and using the log-rank method the survival curves comparisons and hypothesis was tested. Differences between groups were considered statistically significant at  $P < 0.05$ .

#### Cytotoxicity and genotoxicity of the phyto-fabricated silver nanoparticle

**Cell sample preparation:** Lymphocytes were isolated from the bone marrow of the secondary AML mice using Histopaque 1077 (Sigma–Aldrich, St. Louis, MO, USA) following the methodology of Thorsby [27] with modifications. The isolated leukemic lymphocytes were incubated with different concentrations of the green silver nanoparticle (10 µg/ml, 20 µg/ml, 40 µg/ml and 80 µg/ml) and standard drug doxorubicin (at a concentration of 1 µM) in RPMI-1640 media for 3 hour at 37°C. Normal lymphocyte cells treated with highest concentration nanoparticle was the control system.

**Cell viability assay:** Cell viability was checked by Trypan blue exclusion method described by Tennant [28]. 0.4% solution of Trypan blue in buffered isotonic salt solution, pH 7.2 to 7.3 (i.e., phosphate-buffered saline) was added to 1 ml of cell suspension ( $10^6$  cells/ml). Cell viability should be at least 95% for healthy log-phase. The percent of viable cells was calculated using the formula: % of viable cells =  $[1.00 - (\text{Number of blue cells} \div \text{Number of total cells})] \times 100$

**Determination of nitric oxide (NO):** Nitric oxide basically generates from sodium nitroprusside and it is measured by the Griess reaction [29]. Nitric oxide was generated by chemical reaction of sodium nitroprusside. The incubation time was five hours so that the part of the generated nitric oxide was scavenged. The amount of the left over nitric oxide was calculated. The absorbance of the chromophore was then measured at 546 nm. Percentage of scavenging activity =  $(\text{O.D. of control} / \text{O.D. of test}) \times 100$

**ROS generation– DCFDA assay:** The generation of ROS was detected by 2, 7-dichlorofluorescein di-acetate (DCFH-DA) fluorescence. The cell suspension containing approximately  $10^6$  cells per tube was taken for the flow cytometric analysis. The generation of ROS was detected following the methodology of Roy et al. [30]. The samples were untreated stained cells, silver nanoparticle treated cells, positive control cells (treated with hydrogen peroxide) as well as blank tubes containing buffer only. DCF was excited by the 488 nm laser and detected at 535 nm (typically FL1). Ideally 10,000 cells were analyzed per experimental condition.

Mean fluorescent intensity change between control and treated samples was also determined.

**Determination of Mitochondrial Membrane Potential:** Change in the mitochondrial transmembrane potential was determined following the methodology of Dash et al. [31] by flow cytometry at the single-cell layer. The control and treated cells were stained with the dye DiOC6 by incubating for 15 min at 37°C in complete dark in phosphate buffer saline. Loss of DiOC6 fluorescence indicates the disruption of the mitochondrial inner transmembrane potential. The fluorescence was detected at excitation wavelength of 488nm and emission wavelength of 530nm. The fluorescence intensity was measured on a FACS Calibur (Becton Dickinson), and data were analyzed using WINMDI 2.9 software, representing the mean fluorescence intensity.

**DAPI:** Analysis of nuclear membrane integrity of both control and treated cells were performed by DAPI (4', 6-diamidino-2-phenylindole) following the methodology of Mollick et al. [32]. Cells were exposed to 300 nM DAPI stain solution. Cells were imaged under fluorescence microscope at 340 nm.

**Analysis of apoptotic and necrotic cells:** Alexa Fluor® 488 annexin V and Propidium Iodide (Invitrogen) assay was performed according to the manufacturers protocol to quantify the number of apoptotic and necrotic cells. After staining with Alexa Fluor® 488 annexin V and PI the apoptotic cells show green fluorescence, dead cells show red and green fluorescence, and live cells show little or no fluorescence. The cells were washed in cold Phosphate-Buffered Saline (PBS). Finally 5 µl Alexa Fluor® 488 annexin V and 1 µl 100 µg/ml of PI working solution was added to each 100 µl of cell suspension. The stained cells were analyzed by flow cytometry at excitation wavelength of 488 nm; the fluorescence was measured at the emission wavelength of 530 nm and 575 nm (or equivalent).

**Comet Assay:** Analysis of the extent of DNA damage was assessed by comet assay following the methodology of Sing NP (1988) [33]. Following unwinding, the DNA is electrophoresed and stained with a fluorescent dye. DNA migration was analyzed by fluorescence microscopy (excitation filter 515-560 nm and barrier filter of 590 nm) attached with a CCD camera. The images were analyzed by the by Komet version 5.5 auto image analysis software. Quantitative and qualitative analysis of DNA damage was determined by measuring the length of DNA migration and the percentage of migrated DNA in the cells to calculate the tail length.

**DNA fragmentation assay:** DNA was extracted from both the leukemic lymphocyte cells and control cells following the protocol suggested by Paul et al. [34]. After the treatment the cells were lysed and DNA was extracted with a mixture of phenol, chloroform, and isoamyl alcohol (25:24:1) and electrophoretically separated on a 2% agarose gel containing 1 µg/ml ethidium bromide and visualized under ultraviolet transillumination.

**Study of cellular uptake and accumulation by TEM:** A modified cytotoxicity test with AML cells treated with green AgNPs was carried out by TEM imaging following the methodology of AshaRani et al. [35] for the qualitative assessment. Embedded samples were fixed with 2% glutaraldehyde and then post fixed with 2% osmium tetroxide. Ultrathin sections were cut with glass knives and examined in a Zeiss EM910 transmission electron microscope at an acceleration voltage of 80 kv.

## Results

### Survivability Assay

Figure 1(A) represents the percent survivability differences among the different groups of mice. It was evident that at the end of 35 days of study period the survivability of the secondary AML mice was significantly increased ( $p \leq 0.05$ ) in both the groups i.e. the group treated with 43mg/kg b.w and 86mg/kg b.w. of the bio-fabricated silver nanoparticles. The control group of mice was without any effect with 100% survivability whereas the diseased group showed only 17% of survivability. Mice treated with AgNPs at dose of 43mg/kg b.w. revealed increase in percent survivability by 33% whereas at dose of 86mg/kg b.w. the percent survivability was increased by 50% in comparison to that of untreated diseased group. Mice treated with standard drug at a dose of 2mg/kg b.w. showed maximum i.e. 83% of survivability (Figure 1).

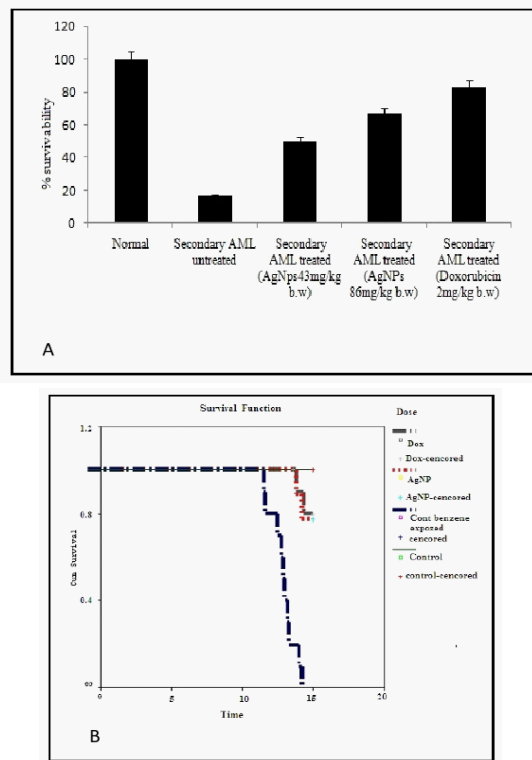


**Figure 1:** Percent survivability differences among different groups of animals. B Survival of mice exposed to benzene and treated with AgNPs and Doxorubicin. The data are presented in a Kaplan Meier format showing the cumulative survival of mice at different time (weeks) points.

**Cytotoxicity and genotoxicity of the phyto-fabricated silver nanoparticles in leukemic lymphocytes**

**Cell viability test by Trypan blue exclusion method:** The cell viability of the leukemic lymphocyte cells (Figure 2E) treated with different concentrations (10µg/ml, 20µg/ml, 40µg/ml and 80µg/ml) of the phyto-fabricated silver nanoparticle was determined and compared with the viability of cells treated with standard drug doxorubicin (at a concentration of 1 µM). The viability of leukemic lymphocyte cells was reduced by 89.14% at maximum concentration of the green silver nanoparticle. The percent of viability reduced by 91.23% in doxorubicin treated leukemic lymphocytes. So there was significant (p<0.05) decrease of percent viability of leukemic lymphocytes, when treated with different concentration of phyto-fabricated silver nanoparticle in a dose dependent manner.

**No release level:** The degree of release of NO is one of the important parameters to analyze the anticancer potentiality of any compound. In the present study we found that at higher concentration (80µg/ml) the phyto-fabricated silver nanoparticles were able to significantly (p<0.05) increase the Reactive Nitrogen Species (RNS) through NO level by 63.4% in the leukemic lymphocyte cells as compared to the control and the value was close to the level of NO (68.7%) in the leukemic lymphocytes treated with the standard drug doxorubicin (Figure 2D). In case of leukemic cells if there is elevated level of NO then it can be assumed that it may be due to severe oxidative injury, which in turn helps in killing the leukemic cells. It is a well known fact that NO reacts with superoxide to form peroxynitrite (ONOO<sub>2</sub>), which is more toxic and has microbicidal and tumoricidal effect. No significant increase in the level of NO was found in the normal cells that were treated with highest concentration of phyto-fabricated silver nanoparticles.

**ROS generation– DCFDA assay:** The generation of ROS was measured in the leukemic lymphocyte cells treated with AgNPs with help of a cell permeable fluorescent dye (2’7’-dichloro fluorescein diacetate DCF-DA) and the outcomes were analyzed in FACS (BD BIOSCIENCE). In the present study, during the analysis we found that the intracellular concentration of ROS (Figure 2A) was significantly (p<0.05) higher in the leukemic lymphocytes treated with the highest concentration (80µg/ml) of the phyto-fabricated silver nanoparticles when compared to the control. Figure 2C represents the fold change variation in generation of ROS in different set of cells. In phyto-fabricated silver nanoparticle treated cells the ROS was elevated by 53.7% (2.26 fold compared to control) and in doxorubicin treated cells the ROS was elevated by 66.76% (2.81 fold compared to control).

**Alteration in mitochondrial membrane potential (MMP)**

In this study the mitochondrial membrane potential (MMP) was measured to determine the cytotoxic effect of the phyto-fabricated silver nanoparticles in the leukemic lymphocyte cell population. When the cell is dead or apoptotic the mitochondrial membrane integrity is diminished but in case of live cells the integrity remains intact. In this study, the MMP of the leukemic lymphocytes treated with AgNPs was found to be depleted significantly in comparison to the control lymphocytes; similar depletion was also found in the doxorubicin treated leukemic lymphocyte cells. The decrease in the percentage of MMP was found to occur in a dose dependent manner i.e. at highest concentration of phyto-fabricated AgNPs the decrease in MMP was maximum i.e. 72.7% which is significantly (P <0.05) higher in comparison to the control. Depletion of MMP as fold change is represented in Figure 2B.

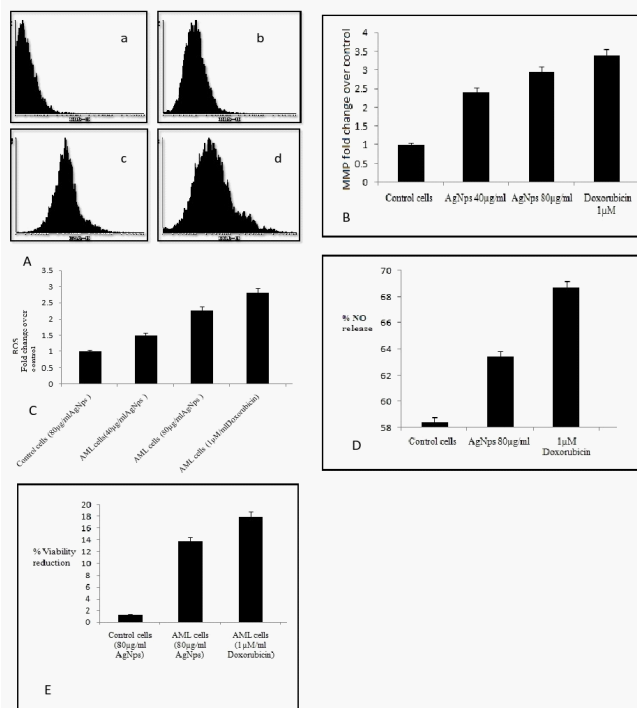


**Figure 2:** A. Generation of ROS. A. a. control cells with high conc. Of AgNP; (b) leukemic lymphocytes treated with AgNPs (40µg/ml); (c) leukemic lymphocytes treated with AgNP (80µg/ml); (d) leukemic lymphocytes treated with standard drug doxorubicin (1µM); B. Fold change in depletion of mitochondrial membrane potential C. Fold change of ROS generation in different set of leukemic lymphocytes. D. NO level in the leukemic lymphocytes in nanoparticle and standard drug treated groups as compared to the control E. The reduction in percent of viable cells in leukemic lymphocytes.

**Fluorescence study by DAPI staining:** With other cytotoxic effects as discussed above, chromatin condensation, cell blebbing, was also investigated by DAPI staining. Imaging of cells after staining with DAPI revealed chromatin condensation and fragmentation in leukemic lymphocytes treated with the highest concentration (80µg/ml) of synthesized silver nanoparticle (Figure 3A). Similar change in the nuclear material was also observed in leukemic cells treated with the standard chemotherapeutic drug doxorubicin (Figure 3). But control cells that is normal lymphocytes treated with highest concentration of phyto-fabricated silver nanoparticle showed no typical characteristics of apoptosis such as nuclear condensation or cell blebbing (Figure 3A.a).

In the analysis we found that there was significant ( $p < 0.05$ ) increase in both apoptosis and necrosis in the leukemic lymphocyte cell population after the treatment with synthesized phyto-fabricated silver nanoparticles (Figure 3B). Result was similar in case of doxorubicin treated leukemic lymphocyte cell population. A significant increase in the number of necrotic cells was observed at the highest concentration of phyto-fabricated silver nanoparticle. Experimental findings also revealed the percentage of leukemic lymphocytes at different phages of cell death viz. live cells, early apoptotic, late apoptotic and necrosis after treatment with phyto-fabricated AgNPs and standard drug doxorubicin (Figure 3C). The significant increase in apoptosis and necrosis of the leukemic lymphocytes is assumed to be contributed by oxidative stress by the phyto-fabricated AgNPs which is in agreement with the other lines of investigations.

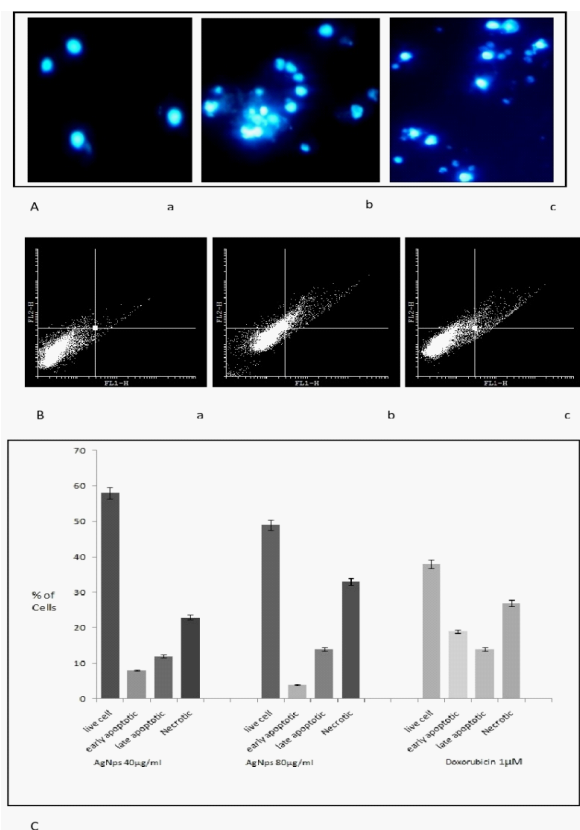


**Figure 3:** Tests of cytotoxicity by staining with DAPI. A. a. Control cells after treatment with phyto-fabricated AgNPs; (b, c) leukemic lymphocytes after treatment with phyto-fabricated AgNPs and doxorubicin respectively; B. Assessment of apoptosis and necrosis (a) Control cell (with AgNPs); (b) after treatment with AgNPs (80µg/ml); (c) leukemic lymphocytes treated with standard chemotherapeutic drug doxorubicin. C. Comparison among the percentage of leukemic lymphocytes at different phages of cell death viz. live cells, early apoptotic, late apoptotic and necrosis.

**Estimation of DNA damage by Comet and DNA fragmentation Assay**

After the treatment with the phyto-fabricated the leukemic lymphocytes were observed for damaged DNA by comet assay. The quantification of the damaged DNA was determined by comparing the tail length of the comet between the leukemic lymphocyte cells treated with green silver nanoparticle with the control cell population (Figure 4A). A significant ( $p < 0.05$ ) increase in DNA damage was observed in both phyto-fabricated silver nanoparticle (at a concentration of 80µg/ml) and doxorubicin treated leukemic lymphocytes (Figure 4B). In the green AgNPs treated AML cells the value of tail length of DNA was approximately 11 fold higher whereas in doxorubicin treated cells it was 14 fold higher than the value of comet obtained in the control cells (normal lymphocytes treated with phyto-fabricated AgNPs) (Figure 4C).

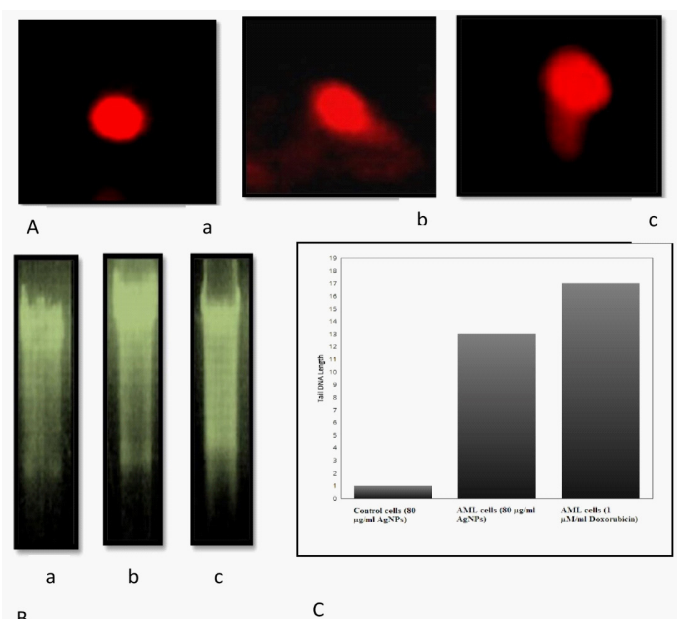


**Figure 4:** Length of comet tail A. (a) control cells (without AgNPs); (b,c) leukemic lymphocytes treated with phyto-fabricated silver nanoparticle and standard drug doxorubicin respectively B. Fragmentation of DNA. a. Control cells; b, c, treatment as before respectively C. Tail length analyzed by Comet assay.

**Study of uptake and structural alterations of AML cells by TEM:** AML cells incubated with phytocfabricated AgNPs (80µg/ml) were evaluated for structural alterations and phytocfabricated AgNPs accumulation. AML cells incubated with green AgNPs were characterized by different degrees of deformities like damaged cell membrane, extensive vacuolation and vesicular degeneration. Features like loss of nuclear organization with ruptured plasma membrane and shrinkage of the protoplast (Figure 5a) were observed in sets of AML cells that were exposed to green AgNPs. Localization of nanoparticles was observed in the vesicles (Figure 5e) of the cells. Extensive vacuole formation (Figure 5d) and lysosomes with partly degraded content (Figure 5c) were also observed.

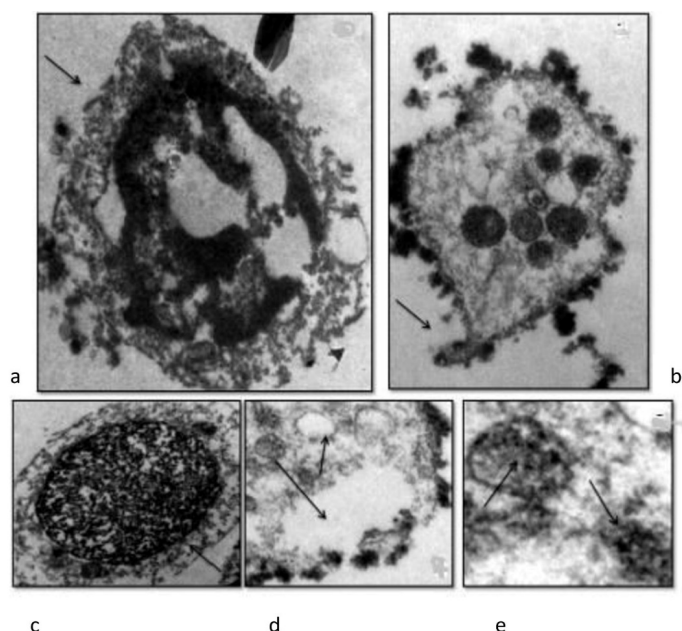


**Figure 5:** Uptake and structural organization of AML cells (a) treated AML with loss of nuclear organization, ruptured plasma membrane and degraded protoplast; (b) AML cells with pseudopodia; (c) lysosome with partly degraded content; (d) extensive vacuolation in the cell; (e) localization of nanoparticles inside the vesicles.

### Discussions

A very few reports are available on the efficacy of green silver nanomaterial in treatment of AML cells [20, 21]. We have developed eco-friendly, phyto-fabricated silver nanoparticles using the aqueous bark extract of the plant *Saraca asoca* following the green chemistry method [24]. The average range of particle size calculated using Dynamic Light Scattering measurements (DLS) was found to be 3-10 nm [24]. AFM analysis showed the presence of almost spherical shaped particles within the size range of <5 nm. FTIR analysis indicated the involvement of carboxyl (-C=O), hydroxyl (-OH) and amine (-NH) functional groups of the phytochemicals in capping and stabilizing silver nanoparticles. The capping and/or stabilizing materials are phyto-compounds like 1, 2, 4-triazole and diethyl acetylenedicarboxylate with relatively higher abundance (data not shown). The rapid electrokinetic behavior of the silver was evaluated using zeta potential (approx -23.2 mV) confirmed its stability [24].

The therapeutic efficacy of the synthesized phyto-fabricated silver nanoparticle [23,36,37] revealed that the percent survivability was increased by 50% in comparison to that of untreated group of AML mice whereas mice treated with standard drug doxorubicin (2mg/kg b.w.) showed 83% survivability (Figure 1A). In this study we demonstrated for the first time that phytofabricated silver nanoparticles could effectively increase the survival distributions like the standard chemotherapeutic drug *in vivo*. The extent of cytotoxicity and genotoxicity of the phyto-fabricated silver nanoparticle was compared between the normal lymphocytes and AML cells *in vitro* to confirm the target specific toxicity of the capped nanoparticle as reported by Netchareonsirisuk et al. [38]. We also confirmed the dose dependent toxicity of the synthesized phyto-fabricated silver nanoparticle in AML cells (Figure 3). Previous evidences were available stating that exposure to AgNPs at different concentration can cause dose-dependent toxicity by inducing oxidative stress and DNA damage which ultimately leads to cell death [39].

The result of trypan blue exclusion method also revealed (Figure 3A) the dose dependent toxicity of the green AgNPs as the reduction in percent of viability of leukemic lymphocytes was increased from 50 to 89.14 % at the highest concentration i.e. at 80µg/ml whereas normal lymphocytes treated at a concentration of 80µg/ml showed no significant reduction. This finding certainly confirmed the cell specific cytotoxicity of the synthesized phytofabricated silver nanoparticle. Many researchers showed evidence that silver nanoparticles can cause DNA damage and stimulate oxidative stress to those cells which lack in their capacity to repair damaged DNA or other oxidative stress [39]. In our study nanosilver with their phyto-chemical capping on its surface inhibited the viability of the cells by inducing oxidative stress. The presence of triazole is assumed to have induced the cytotoxicity of AgNPs as it has proven anti-cancerous activity against a wide range of cancerous cells [40]. So the potential vulnerability of the AML cells to the cytotoxicity of the synthesized green silver nanoparticle can be exploited to develop this green AgNPs as a new therapeutic agent in AML treatment.

The elevated production of NO in the cell after exposure to silver nanoparticle is also crucial in asserting its cytotoxic ability because in reaction with superoxide NO usually produces more toxic peroxynitrite (ONOO<sup>-</sup>) which attributes to severe oxidative damage leading to cell death [31]. In our study, NO level in the leukemic lymphocyte cells was 63.4% which was close to value of doxorubicin treated AML cells where the value was 68.7% (Figure 2D). No significant increase of NO was found in the control cells treated with the green AgNPs (data not shown). Thus the elevated level of NO in the green AgNPs treated leukemic lymphocytes contributed in the severe oxidative injury leading to the death of AML cells.

One possible mechanism to induce cell death is by promoting the generation of ROS. Normal cellular growth and its survival are controlled by maintaining a homeostasis in cellular ROS [41]. By estimating the amount of intracellular ROS the vulnerability of the cell to oxidative stress can be determined. In our study generation of ROS was elevated by 2.26 fold (53.7%) after exposure to synthesized silver nanoparticle (Figure 2C) in comparison to the control where the production of ROS was moderate (23.76%). Excessive amount of ROS attributes to cell death by two pathways either apoptosis or necrosis. In our study, significant ( $p < 0.05$ ) elevation of ROS in AML cells (Figure 2A, C) after treatment with AgNPs is due to the cytotoxic efficacy of the synthesized green AgNPs. The toxic effect of nanoparticles is due to its small size (<5nm) and power of penetration of biological membrane barriers to reach different organs. On the other hand surface functionalization by the phyto-components increased the chemical reactivity inside the cell leading to excess generation of ROS [42].

The apoptotic cells can be identified by the loss of mitochondrial membrane integrity though in living cells the mitochondrial membrane integrity remain unchanged. The percentage of MMP decreased significantly ( $P < 0.05$ ) with the increase in the concentration of AgNPs. After treatment with phytofabricated silver nanoparticle the depletion in MMP was 2.4 fold at 40µg/ml concentration, 2.95 fold at 80µg/ml concentration and in doxorubicin treated cells it was 3.4 fold (Figure 2B). The dissipation in MMP in the AgNPs exposed AML cells are assumed to be disrupted of their mitochondrial membrane.

The quantification of the percent of apoptosis and necrosis also revealed that the phyto-fabricated silver nanoparticles was

toxic to the AML cells in a dose dependent manner, at highest concentration of green AgNPs the percent of apoptotic cells were increase by 1.5 fold in comparison to control (Figure 3C), again the percent of necrosis was higher than apoptosis in this group of cells. After exposure the increase in ROS and subsequent decrease in mitochondrial membrane potential might be the reason behind the induction of apoptosis and necrosis in the green Ag NPs treated cells. DAPI staining and imaging of the AML cells showed condensed and fragmented chromatin as well as cell blebbing in AML cells after treatment with nanoparticles, similar result was obtained when AML cells were treated with doxorubicin indicating that the synthesized phyto-fabricated silver nanoparticle was also able to induce death of leukemic cells like that of standard chemotherapeutic drug (Figure 3A). The disruption in chromatin structure contributes to cell death by turning on the apoptotic process [32]. Comet tail length of the AML cells treated with AgNPs and doxorubicin in comparison with control cells concurrent this observation. The value of tail DNA was approx. 11 fold higher than the control whereas in doxorubicin treated cells it was approx. 14 fold higher (Figure 4A). The presence of comet tail was due to the oxidative attack causing DNA damage which was attributed by the cytotoxic effect of the green silver nanoparticle. The damage of the cellular architecture was shown by TEM images of the AML cells treated with phytofabricated silver nanoparticles. The damage was due to morphological alterations, extensive vacuolation, loss of nuclear organization, ruptured plasma membrane, partly degradation of lysosome contents, and shrinkage of the protoplast (Figure 5) associated with apoptotic/necrotic cell death induced by the phytofabricated AgNPs after internalization into the cellular vesicles. These findings thus confirmed the uptake of green AgNPs by the AML cells and also the induced cytotoxicity due to oxidative damage.

### Summary

we demonstrated that the synthesized phyto-fabricated silver nanoparticle has a unique selective toxicity profile. Furthermore we found in our study that the phyto-fabrication reduced the toxicity of the nanoparticle itself on normal cells and capping materials imposed the chemopreventive potential on AgNPs in an environmentally sustainable pathway.

### Acknowledgement

The authors gratefully acknowledge DST-PURSE programme, Government of India for funding this project.

### Author contributions

The concept, design of the experiments to solve the problem was framed by the authors. Data acquisition, literature search for the framing of manuscript was done by the first and second authors. All the authors have contributed in data analysis, statistical analysis, and manuscript editing and review process. D. Nath as the corresponding author is the guarantor for the integrity of the work as a whole.

### References

1. Scott EN, Gescher AJ, Steward WP, Brown K. Development of dietary phytochemical chemopreventive agents: Biomarkers and choice of dose for early clinical trials. *Cancer Prev Res (Phila)*. 2009; 2: 525-530.
2. Hu ML. Dietary polyphenols as antioxidants and anticancer agents: more questions than answers. *Chang Gung Med J*. 2011; 34: 449-460.
3. Cragg GM, Newman DJ. Plants as a source of anticancer agents. *J Ethnopharmacol*. 2005; 100: 72-79.
4. Balunas MJ, Kinghorn AD. Drug discovery from medicinal plants. *Life Sci*. 2005; 78: 431-441.
5. Liu RH. Potential synergy of phytochemicals in cancer prevention: mechanism of action. *J Nutrition*. 2004; 134: 3479S-3485S.
6. Prabhu D, Arulvasu C, Babu G, Manikandan R, Srinivasan P. Biologically synthesized green silver nanoparticles from leaf extract of *Vitex negundo* L induce growth-inhibitory effect on human colon cancer cell line HCT15. *Proc Biochem*. 2013; 48: 317-324.
7. Krishnaraj C, Muthukumaran P, Ramachandran R, Balakumaran M, Kalaichelvan P. *Acalypha indica* Linn: Biogenic synthesis of silver and gold nanoparticles and their cytotoxic effects against MDA-MB-231 human breast cancer cells. *Biotech Rept*. 2014; 4: 42-49.
8. Gurunathan S, Han JW, Eppakayala V, Jeyaraj M, Kim JH. Cytotoxicity of biologically synthesized silver nanoparticles in MDA-MB-231 human breast cancer cells. *Biomed Res Int*. 2013; 96: 53-57.
9. Elangovan K, Elumalai D, Anupriya S, Shenbhagaraman R, Kaleena P, et al. Phyto mediated biogenic synthesis of silver nanoparticles using leaf extract of *Andrographis echinoides* and its bio-efficacy on anticancer and antibacterial activities. *J Photochem Photobiol B: Biol*. 2015; 151: 118-124.
10. Arunachalam KD, Annamalai SK, Arunachalam AM, Kennedy S. Green synthesis of crystalline silver nanoparticles using *Indigofera aspalathoides*-medicinal plant extract for wound healing applications. *As. J Chem*. 2013; 25: S311-S314.
11. Paul JAJ, Selvi BK, Karmegam N. Biosynthesis of silver nanoparticles from *Premna serratifolia* L leaf and its anticancer activity in CCl<sub>4</sub>-induced hepato-cancerous Swiss albino mice. *Appl. Nanosci*. 2015; 5: 937-944.
12. Sre PRR, Reka M, Poovazhagi R, Kumar MA, Murugesan K. Antibacterial and cytotoxic effect of biologically synthesized silver nanoparticles using aqueous root extract of *Erythrina indica* lam. *Spectrochimica Acta Part A: Mol Biomol Spectroscop*. 2015; 135: 1137-1144.
13. Sukumar UK, Bhushan B, Dubey P, Matai I, Sachdev A, et al. Emerging applications of nanoparticles for lung cancer diagnosis and therapy. *Int Nano Lett*. 2013; 3: 45-17.
14. Pardhasaradhi BVV, Reddy M, Ali AM, Kumari, AL, Khar A. Antitumour activity of *Annona squamosa* seed extracts is through the generation of free radicals and induction of apoptosis. *Ind J Biochem Biophys*. 2004; 41: 167-172.
15. Chen WY, Chang FR, Huang ZY, Chen JH, Wu YC, et al. Tubocapsenolide: A novel withanolide inhibits proliferation and induces apoptosis in MDA-MB-231 cells by thiol oxidation of heat shock proteins. *J Biol Chem*. 2008; 283: 17184-17193.
16. Fleischauer AT, Poole C, Arab L. Garlic consumption and cancer prevention: meta-analyses of colorectal and stomach cancers. *Am J Clin Nutrition*. 2000; 72: 1047-1052.
17. Ishikawa H, Saeki T, Otani T, Suzuki T, Shimozuma K, et al. Aged garlic extract prevents a decline of NK cell number and activity in patients with advanced cancer. *J Nut*. 2006; 136: 816S-820S.
18. Wilken R, Veena MS, Wang MB, Srivatsan ES. Curcumin: a review of anti-cancer properties and therapeutic activity in head and neck squamous cell carcinoma. *Mol. Cancer*. 2011; 10: 1-19.
19. Dhillon N, Aggarwal BB, Newman RA, Wolff RA, Kunnumakkara, AB, et al. Phase II trial of curcumin in patients with advanced

- pancreatic cancer. *Clinical Cancer Res.* 2008; 14: 4491-4499.
20. Guo D, Zhu L, Huang Z, Zhou H, Ge Y, et al. Anti-leukemia activity of PVP-coated silver nanoparticles via generation of reactive oxygen species and release of silver ions. *Biomaterials.* 2013; 34: 7884–7894.
  21. Guo D, Zhao Y, Zhang Y, Wang Q, Huang Z, et al. The cellular uptake and cytotoxic effect of silver nanoparticles on chronic myeloid leukemia cells. *J Biomed Nanotechnol.* 2014; 10: 669-678.
  22. Roy I, Das B, Rahaman Mollick M, Basu A, Dey A, et al. Nanotherapy on human acute myeloid leukemia cells using RGO/Ag nanocomposites. *RSC Adv.* 2016; 6: 52403-52410.
  23. Saha S, Mukhopadhyay MK, Ghosh PD, Nath D. Effect of methanolic leaf extract of *Ocimum basilicum* L on benzene-induced hematotoxicity in mice. *Evidence Based Complement Alternate Med.* 2012; 176-385.
  24. Banerjee P, Nath DA. Phytochemical Approach to Synthesize Silver Nanoparticles for Non-Toxic Biomedical Application and Study on their Antibacterial Efficacy. *Nanosci Technol.* 2015; 2: 1-14.
  25. OECD. Test guideline 425. Acute Oral toxicity test: the up and down procedure. In: *OECD guidelines for the testing of chemicals.* Paris, France: Organization for Economic Cooperation and Development. Organization for Economic Cooperation & Development (OECD). 2001.
  26. Kaplan EL, Meier P. Nonparametric estimation from incomplete observations. *J. Amer. Statist. Assn.* 1958; 53: 457-481.
  27. Thorsby E, Bratlie A. A rapid method for preparation of pure lymphocyte suspensions. *Histocompatibility Testing, Terasaki, P.I., ed.,* 1970; 665-666.
  28. Tennant JR. Evaluation of the trypan blue technique for determination of cell viability Transplantation. 1964; 2: 685-694.
  29. Sreejayan N, Roa MNA. Nitric oxide scavenging by curcuminoids. *J Pharm Pharmacol.* 1997; 49: 105-107
  30. Roy A, Ganguly A, Dasgupta S, Das BB, Pal C, et al. Mitochondria-dependent reactive oxygen species-mediated programmed cell death induced by 33-diindolylmethane through inhibition of FOF1-ATP synthase in unicellular protozoan parasite *Leishmania donovani*. *Mol. Pharmacol.* 2008; 74: 1292-1307.
  31. Dash SK, Chattopadhyay S, Ghosh T, Tripathy S, Das S, et al. Antileukemic efficacy of monomeric manganesebased metal complex on KG-1A and K562 cell lines. *ISRN Oncol.* 2013; 69: 70-92.
  32. Mollick MMR, Bhowmick B, Mondal D, Maity D, Rana D, et al. Anticancer (in vitro) and antimicrobial effect of gold nanoparticles synthesized using *Abelmoschus esculentus* (L) pulp extract via a green route. *RSC Adv.* 2014; 4: 37838-37848.
  33. Singh NP, McCoy MT, Tice RR, Schneider EL. A simple technique for quantification of low levels of DNA damage in individual cells. *Exp Cell Res.* 1988; 175: 184-191.
  34. Paul S, Bhattacharyya SS, Samaddar A, Boujedaini N, Khuda-Bukhsh AR. Anticancer potentials of root extract of *Polygala senega* against benzo-pyrene-induced lung cancer in mice. *J Chin Integr Med.* 2011; 9: 320-327.
  35. AshaRani PV, Low Kah Mun G, Hande MP, Valiyaveetil S. Cytotoxicity and genotoxicity of silver nanoparticles in human cells. *ACS Nano.* 2009; 3: 279-290.
  36. Akbay P, Basaran AA, Undeger U, Basaran N. In vitro immunomodulatory activity of flavonoid glycosides from *Urtica dioica* L. *Phytother Res.* 2003; 17: 34-37.
  37. Mukhopadhyay M, Shaw M, Nath D. Chemopreventive potential of major flavonoid compound of methanolic bark extract of *Saraca asoca* (Roxb) in benzene -induced toxicity of acute myeloid leukemia mice. *Pharmacogn. Mag.* 2017; 13: 216-223.
  38. Netchareonsirisuk P, Puthong S, Dubas S, Palaga T, Komolpis K. Effect of capping agents on the cytotoxicity of silver nanoparticles in human normal and cancer skin cell lines. *J Nanoparticle Res.* 2016; 18: 322.
  39. Lim HK, Asharani PV, Hande MP. Enhanced genotoxicity of silver nanoparticles in DNA repair deficient Mammalian cells. *Front Genet.* 2012; 3: 104.
  40. El-Sherief HAM, Youssif BGM, Bukhari SNA, Abdel-Aziz M, Abdel-Rahman HM. Novel 1,2,4-triazole derivatives as potential anticancer agents: Design, synthesis, molecular docking and mechanistic studies. *Bioorg Chem.* 2018; 76: 314-325.
  41. Trachootham D, Alexandre J, Huang P. Targeting cancer cells by ROS-mediated mechanisms: A radical therapeutic approach? *Nat Rev Drug Discov.* 2009; 8: 579-591.
  42. Khorrami S, Zarrabi A, Khaleghi M, Danaei M, Mozafar MR. Selective cytotoxicity of green synthesized silver nanoparticles against the MCF-7 tumor cell line and their enhanced antioxidant and antimicrobial properties *Int J Nanomedicine.* 2018; 13: 8013-8024.